UC Santa Cruz
UC Santa Cruz Previously Published Works

Title

Automatic Contour-Based Road Network Design for Optimized Wind Farm Micrositing

Permalink

https://escholarship.org/uc/item/431720b4

Journal

IEEE Transactions on Sustainable Energy, 6(1)

ISSN

1949-3029

Authors

Gu, Huajie
Wang, Jun
Lin, Qin
et al.

Publication Date

2015

DOI

10.1109/tste.2014.2369432

Peer reviewed

Automatic Contour-Based Road Network Design for Optimized Wind Farm Micrositing

Huajie Gu, Jun Wang, *Senior Member, IEEE*, Qin Lin, and Qi Gong

Abstract—Constructing the access roads between wind turbines requires a significant cost when a wind farm is built in hills or mountains. An optimized design of road network can substantially reduce construction costs and increase investment returns. In this paper, we consider a challenging problem of the road network design for a wind farm with complex topography. An automatic contour-based model is developed for road network design, and is incorporated into the optimization of wind farm micrositing to maximize investment returns of the wind farm. The directions of access roads are first deduced from a contour tree, the route projections are then designed by a gradient-bounded algorithm, and the most cost-effective road network is finally obtained by the minimum spanning tree algorithm. The topographic speedup, wind resource grid and Park wake model are incorporated to accurately evaluate the power production of the wind farm. Both the profit of wind energy sales and the cost of access roads are combined into a cost function called net present value, which is optimized using genetic algorithms. Simulation results illustrate that the length of access roads is decreased significantly while the locations of wind turbines are optimized. The proposed method simultaneously optimizes the turbine layout and road network of the wind farm, therefore achieving a more practical and profitable wind farm micrositing.

Index Terms—Access roads, contour tree, micrositing, road network, wind farm.

NOMENCLATURE

α	Wake decay constant.
δ_{xyi}	Topographic speedup or speeddown of wind in the ith direction at the location (x, y).
Δh_c	Contour interval.
Δv	Wake deficit.
κ_i	Shape parameter of Weibull distribution in the ith wind direction.
λ_i	Scale parameter of Weibull distribution in the ith wind direction.
ρ_i	Frequency of wind occurrence in the ith direction.
A_b	Area of rotor plane of turbine "b".
A_{op}	Overlapping fraction of a wake with a downwind turbine rotor plane.
$\text{AEP}(\boldsymbol{z})$	Annual energy production of a turbine layout $\boldsymbol{z}$.
c_i	Label of the ith node (contour) in a contour tree.
C_t	Turbine thrust coefficient.
D_a	Rotor diameter of turbine "a".
E_{ij}	Edge between the ith node V_i and the jth node V_j in a graph.
$G(\boldsymbol{V}, \boldsymbol{E})$	Complete graph with nodes $\boldsymbol{V}$ and edges $\boldsymbol{E}$.
g_r	Road gradient.
h_{wt}	Hub height of a wind turbine.
$L_{\text{RN}}(\boldsymbol{z})$	Total length of a road network for a turbine layout $\boldsymbol{z}$.
$\text{MST}(\boldsymbol{V}, \boldsymbol{S})$	Optimal road network represented by the minimum spanning tree with nodes $\boldsymbol{V}$ and edges $\boldsymbol{S}$.
N_d	Number of wind sectors (directions) on a wind rose.
N_{gen}	Number of generations in genetic algorithms.
N_{pop}	Population size in genetic algorithms.
N_t	Number of wind turbines.
$P(v)$	Turbine power output at wind speed v.
R	Radius of the auxiliary circle used in route projection.
$T(\boldsymbol{V}, \boldsymbol{U})$	Spanning tree with nodes $\boldsymbol{V}$ and edges $\boldsymbol{U}$.
v	Wind speed.
v_a, v_j	Incident wind speed at turbines "a" and "j", respectively.
v_{in}	Cutin wind speed of a turbine.
v_{out}	Cutout wind speed of a turbine.
$\overline{v}_i$	Mean wind speed for a pair of Weibull parameters κ_i and λ_i.
$\overline{v}_{xyi}$	Mean wind speed in the ith wind direction at the location (x, y).
V_i	ith node of a graph.
W_{c_1, c_M}	Road direction between the contour c_1 and the contour c_M.
x_{ab}	Downwind horizontal distance between turbines "a" and "b".
z_0	Surface roughness length of a wind farm.
$\boldsymbol{z}$	Layout of turbines.

I. INTRODUCTION

WIND ENERGY is nowadays widely used as a promising renewable energy. A wind power generation station, also called a wind farm, usually consists of a large number of wind turbines. Once a suitable site is allocated for a wind farm, empirical or systematical methods can be utilized to optimize

TABLE I
INITIAL INVESTMENT BREAKDOWN OF TYPICAL ONSHORE
WIND FARMS [1]–[5]

Items	Cost percentage (%)
Wind turbines	$65-84$
Civil works	$4-20$
Electrical infrastructure	$9-15$
Other	$4-10$

the turbine layout in terms of energy production and/or financial income by considering the effects of local wind resources, wake effects, terrains, etc.

In the micrositing process, the number and the type of wind turbines, civil works, and electrical infrastructure all influence the economy benefits of a wind farm project. Table I shows the initial investment breakdown of typical onshore wind farms [1]–[5]. As wind turbines account for a major proportion of the wind farm initial investment, previous researches mainly focused on optimizing the number and locations of wind turbines. In [6] and [7], the genetic algorithm was proposed to iteratively optimize gridded turbine layouts on flat terrains. In [8] and [9], the greedy algorithm was introduced to search for the optimal gridded turbine layouts on hilly wind farms. The modified particle swarm optimization algorithm [10] was applied to solve the turbine layout optimization problem in a continuous solution space.

The civil works include the construction of access roads, turbine foundations, crane hard-standings, cable-trenching, and substation buildings. Their cost can be substantial. Access roads are greatly influenced by topographic characteristics, and their cost is much higher for hilly or mountainous wind farms than plain ones [1]. A comparative strategy [2] and the minimum spanning tree [3] were proposed to search for the shortest road network for wind farms in *flat* areas. In [11], the Euclidean Steiner tree was introduced to further reduce the length of the road network. However, these methods are not directly applicable to *hilly* or *mountainous* wind farms where the road gradient must be considered to build winding roads capable of accommodating significant weight.

Wind farms are generally constructed in rural areas with challenging topography. With the rapid expansion of wind farms, new farms have to be built in hills or mountains, where designing suitable access roads for construction, turbine erection and maintenance is not straight forward. It is necessary to know roughly which route should be chosen to connect turbines and how much they will cost, while placing turbines at the peaks for high energy production. The selection of appropriate access roads is essential for the overall planning of the wind farm construction. A well-chosen road network can also reduce the wind farm construction period and lower the environmental impact [12].

In this paper, the constraints on the maximal gradient of access roads are guaranteed when developing an automatic contour-based road-network design model. The design of access roads and the evaluation of their cost are *simultaneously* considered in the process of optimizing turbine layouts, which

results in a more technically feasible and economically beneficial micrositing of wind farms. The remainder of this paper is organized as follows. Section II proposes an automatic model for road network design. The problem of wind farm micrositing is formulated in Section III. Section IV gives the simulation results. Finally, Section V makes some concluding remarks.

II. AUTOMATIC ROAD-NETWORK DESIGN MODEL

The configuration of the road network for accessing the turbines on a farm from its entrance is similar to a tree structure. It can be transferred into an undirected graph by mapping the turbine layout z into the nodes V, and the roads between them into the edges U. Therefore, a solution to the road network is an undirected graph $T(V, U)$, where $V = \{V_1, V_2, \ldots, V_{N_t}\}$, $U = \{U_{12}, U_{13}, \ldots, U_{ij}, \ldots\}$, $i, j \in \{1, 2, \ldots, N_t\}$, $i \neq j$ with N_t be the total number of turbines. The edge U_{ij} of the graph represents the road between the ith and jth turbines. The most cost-effective road network can be found by calculating the corresponding minimum spanning tree with assigned weightings for each edge. For a wind farm on a flat terrain, straight lines directly connecting any two wind turbines can be considered as edges [2], [3]. However, for a wind farm built in hills or mountains, roads are usually polylines or curves, and topographic constraints should be considered in the design so that a feasible route can be built and reasonable road cost can be evaluated.

In civil engineering, a feasible route between the starting and end points is selected by establishing a series of control points on the terrain. Using these control points as an initial alignment, the horizontal and vertical curves are then located, subject to the road design constraints including geometric specifications and environmental requirements. Heuristic optimization algorithms such as the genetic algorithm, the Tabu search, and the simulated annealing algorithm [13]–[15] have been applied to optimize horizontal and vertical alignments of roads. These algorithms depend on a high-resolution digital elevation model to support the analysis of road design features such as ground slopes and other landform characteristics. The calculation of an optimal route between two given locations is time consuming and could even take several hours.

The micrositing optimization process usually involves hundreds or thousands of iterations to evaluate the wake effects between turbines and to update the turbine layout. The process *without* road design is already intensive [2], [3], [6]–[10], [16]. If a complex road network for the whole farm needs to be designed in each iteration by the aforementioned heuristic optimization algorithms, the computation burden is prohibitive and even impossible. In this paper, only the control points of access roads are selected during the micrositing optimization process. Such a relatively simple and functional road design is suitable for low-volume access roads, which are mainly for wind farm construction and maintenance. It is also adequate for the design at the strategic and tactical level. Based on the above assumption, a fast automatic method for road-network design is developed to estimate the cost of access roads during the optimization of wind farm micrositing.

A. Route Projection

Forest engineers usually use large-scale contour maps to select preliminary routes with dividers to connect two locations, a process known as route projection [17]. Control points of a road can be selected during the route projection process. In this paper, contour lines as a group of nested closed curves are chosen to store topographic information of wind farms. A distinct advantage of the contour-line data over a digital elevation model is that the vector representation lends itself to the object-oriented modeling of terrains, which provides a natural mechanism for sorting terrains and facilitates the search through a contour map [18].

Given a technically feasible gradient, a route is projected from the starting point toward the end across adjacent contour lines. This process can be efficiently automated with a mathematical model. The basic idea of the route projection process is to determine the projected route segment between two neighboring contour lines, as the elevation of the terrain rises continuously. Every projected segment of the route must begin from a point on a contour line and end on another one. The next control point is located on an adjacent contour line at a distance [17]

$$R = \frac{\Delta h_c}{g_r}$$

where R is the distance or the divider width between two adjacent contour lines, Δh_c is the contour interval on the topographic map, and g_r is the desired road gradient. The route projection process can be formulated by the following gradient-bounded algorithm:

Step 1) Draw an auxiliary circle with its center at the current control point and a radius R.

Step 2) Find the desirable intersection (next control point) of the auxiliary circle and the next adjacent contour line. If the next control point is found, a new segment of the route is created.

Step 3) Take the intersection as the current control point, and go back to Step 1 to find the next control point. The process stops until the next control point reaches the end point of the road.

Note that, there might be none, one or two intersections in Step 2. In the case of two intersections, only one intersection should be chosen according to the principle of the shortest road length. If none intersections are found, the gradient between these two adjacent contour lines is no greater than g_r. The next control point is just the intersection made by the next adjacent contour line and a straight line connecting the current control point and the end point. The gradient of each route segment is, therefore, no greater than the given gradient g_r.

In each projection iteration, one can easily find the next adjacent contour line by directing the route toward the end point. Fig. 1 illustrates an example of route projection process assisted by auxiliary circles. An automatic process of selecting road directions is formulated in the following section.

B. Road Direction

Roads in hills or mountains are usually built windingly to guarantee feasible gradients. A road direction is based on the
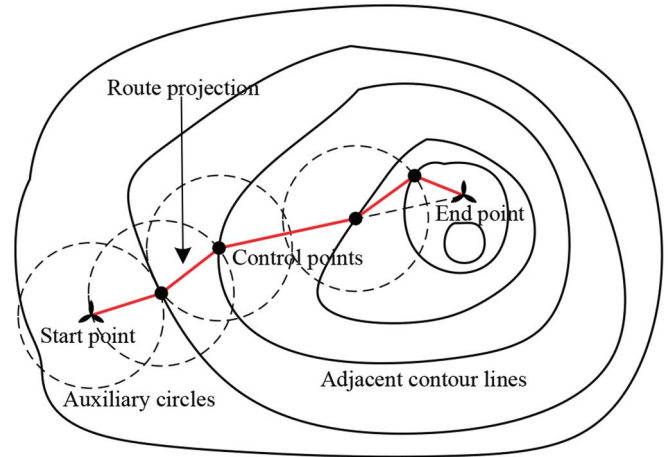

Fig. 1. Example of route projection process.

spatial relations of contour lines, typically from the lines with lower elevations toward the enclosed higher ones. A contour tree is employed to deduce the direction of the route projection between the starting and end points. The contour tree transfers a contour map into an undirected graph by mapping contour lines and their intercontour regions into nodes, and enclosure relationship between contour lines into edges. Each edge connecting two nodes means that the child node is enclosed by its parent node, i.e., the contour line with a lower elevation (the parent node) encloses the higher ones (the children nodes). The contour tree is a labeled tree in which each node is given a unique label representing the corresponding contour line on the contour map. The point-in-polygon method, the region growing method, or the Voronoi interior adjacency method [18] can be utilized to generate a contour tree from a contour map. The point-in-polygon method is used in this paper.

The contour map of a hilly wind farm and the corresponding contour tree is shown in Fig. 2. The elevation of each level in the contour tree is sorted in ascending order. All of the contour lines are sorted according to this order and stored as the nodes of the tree. The level of the tree represents the elevation range of the contour map. The root node has the minimal elevation while the leaf nodes represent local peaks.

The road direction from the starting point to the end one can be represented by the path vector $\boldsymbol{W}_{c_1,c_M}$ consisted of adjacent contour lines crossed by the road

$$\boldsymbol{W}_{c_1,c_M} = [c_1, c_2, \ldots, c_i, \ldots, c_M]$$

where c_i is the label of the ith node representing the corresponding contour line, and M is the total number of the crossed contour lines. Note that c_1 represents the closest contour line encloses the starting point and can be found by the point-in-polygon method [19], while c_M is the closest one encloses the end point. If we assume that the weighting of each edge of the contour tree is equal, $\boldsymbol{W}_{c_1,c_M}$ can be identified by searching for the shortest path between c_1 and c_M. For the example shown in Fig. 2(b), if $c_1 = 4$ and $c_M = 16$, we have $\boldsymbol{W}_{4,16} = [4, 2, 3, 8, 14, 16]$.

Given a road direction, the route projection can be fully automated by the gradient-bounded algorithm given in Section II-A.
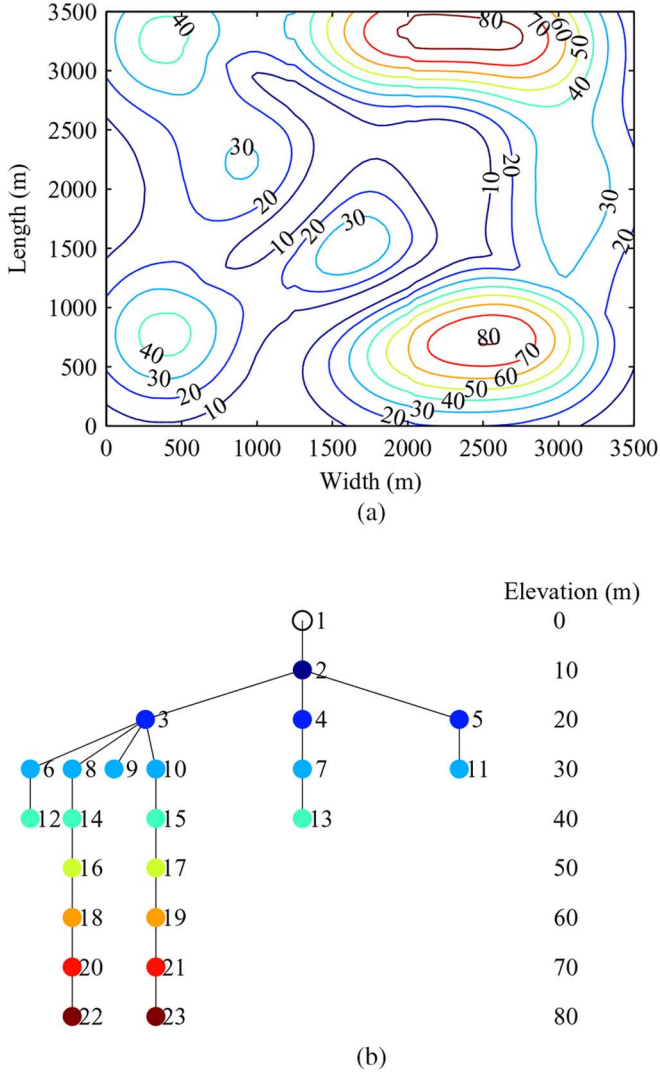
Fig. 2. Contour map and its corresponding contour tree of a wind farm. (a) The contour map. (b) The contour tree.

The whole route from the starting point to the end can be designed by merging adjacent segments together into one long road with a gradient no greater than g_r. In order to reduce the computation burden of the proposed model, the final design for smoothing sharp corners between adjacent segments is ignored in this paper.

C. Road Network

The edge E_{ij} of a pair of distinct nodes V_i and V_j in $\boldsymbol{V}$ can be achieved using the automatic route projection method proposed in Sections II-A and II-B. The complete graph $G(\boldsymbol{V}, \boldsymbol{E})$ of the turbine layout $\boldsymbol{z}$ is then generated, where $\boldsymbol{V} = \{E_{12}, E_{13}, \ldots, E_{ij}, \ldots\}$. The road network $T(\boldsymbol{V}, \boldsymbol{U})$ is a spanning tree of $G(\boldsymbol{V}, \boldsymbol{E})$, where $\boldsymbol{U} \subset \boldsymbol{E}$. It is a subgraph that connects all nodes and contains no cycles. The minimum spanning tree, $\mathrm{MST}(\boldsymbol{V}, \boldsymbol{S})$ of $G(\boldsymbol{V}, \boldsymbol{E})$ where $\boldsymbol{S} \subset \boldsymbol{E}$, of an undirected graph is the spanning tree with minimum total edge cost of all the spanning trees.

In this paper, the length of three-dimensional polyline generated by the route projection is assigned to the weighting of the corresponding edge, and the weighting of a spanning tree is the sum of all the weightings. The Prim algorithm [20] is used to calculate the minimum spanning tree. It grows the minimum spanning tree one edge at a time by adding a minimal weighting edge that connects a node in the growing minimum spanning tree with any other nodes. The total length $L_{\mathrm{RN}}(\boldsymbol{z})$ of the minimum spanning tree and the cost per unit length are used to calculate the cost of access roads for wind farm micrositing optimization.

III. WIND FARM MICROSITING MODELS

A. Topographic Speedup

The distribution of wind directions is usually described by a wind rose. On the rose, the compass is equally divided into several sectors. The length of each sector represents the frequency of wind occurrence in the associated direction. The statistical behavior of wind speed in each direction is represented by the following Weibull probability density function [10]

$$f_i(v) = \frac{\kappa_i}{\lambda_i}\left(\frac{v}{\lambda_i}\right)^{\kappa_i - 1} e^{-\left(\frac{v}{\lambda_i}\right)^{\kappa_i}} \tag{1}$$

where κ_i and λ_i are the shape and scale parameters in the ith wind direction, respectively. The mean wind speed for a given pair of Weibull κ_i and λ_i can be calculated by the following gamma function [21]:

$$\overline{v}_i = \lambda_i \Gamma\left(1 + \frac{1}{\kappa_i}\right). \tag{2}$$

Wind will accelerate near the summit of hills and decelerate near the foot of hills or in valleys. The topographic speedup or speeddown of wind in the ith direction for a given location (x, y) is defined as [21]

$$\delta_{xyi} = \frac{\overline{v}_{xyi}}{\overline{v}_{x_0 y_0 i}} \tag{3}$$

where $\overline{v}_{xyi}$ and $\overline{v}_{x_0 y_0 i}$ are the mean wind speeds at the same height above ground level at the given location (x, y) and the reference location (x_0, y_0), respectively. The speedup is achieved using a wind resource grid calculated with WAsP [21], [22]. The wind resource grid is a table containing the wind rose and the sectorwise Weibull distribution parameters for each regularly spaced point on a wind farm [22].

B. Wake Model

A turbine extracts energy from wind and leaves behind a wake characterized by reduced wind speed. The other turbines operating in this wake will therefore produce less energy. The Park wake model supporting different types of turbines was proposed in [23] and [24] and has been utilized in commercial software such as WAsP [22] and OpenWind [21]. The effects of different hub heights and rotor diameters are taken
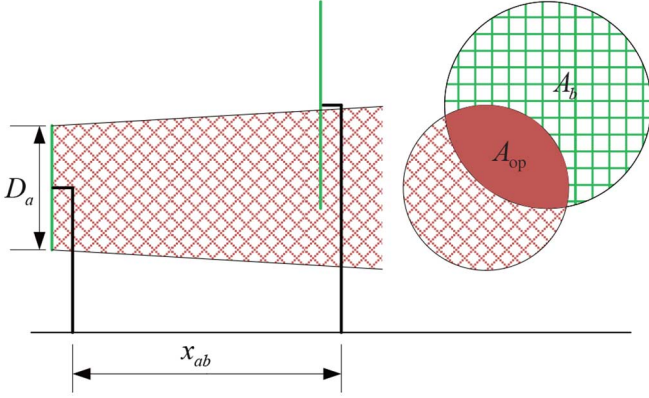
Fig. 3. Park wake model [22].

Fig. 4. Thrust coefficient curve and power curve of UP1500-86 [27], [28].

into account through the overlap A_{op} of a wake and a downwind rotor plane [22]. As indicated in Fig. 3, the wake deficit Δv at the downwind wind turbine b is [22], [24]

$$\Delta v = v_a \left(1 - \sqrt{1 - C_t}\right) \left(\frac{D_a}{D_a + 2\alpha x_{ab}}\right)^2 \frac{A_{\mathrm{op}}}{A_b} \quad (4)$$

where v_a is the incident wind speed at the upwind turbine a with a rotor diameter D_a, C_t is the turbine thrust coefficient, x_{ab} is the downwind horizontal distance between the wind turbines, and α is the wake decay constant. The wake decay constant α sets the linear rate of expansion of the wake with distance downwind and is determined by [25]

$$\alpha = \frac{0.5}{\ln(h_{\mathrm{wt}}/z_0)} \quad (5)$$

where z_0 is the surface roughness length of the wind farm and h_{wt} is the hub height of the wind turbine.

The incident wind speed at a downwind turbine is therefore the free stream wind speed minus the wake deficit. When there are several upstream wind turbines with overlapping wakes, the incident speed is assumed to equal the free stream speed minus the largest single wake deficit [21]. In addition, further downstream turbines may be affected by already wake-affected turbines. The wake generated by a wake-affected turbine is the same as if the turbine were in the free stream except that its thrust coefficient, C_t, is calculated using the incident wind speed for that turbine [21]. This assumption ensures that the wake wind speed at a distance far downstream will recover to the free stream speed rather than the incident one on the rotor [21].

C. Net Present Value

The expected annual energy production $\mathrm{AEP}(\boldsymbol{z})$ of N_t number of turbines can be calculated by [16]

$$\mathrm{AEP}(\boldsymbol{z}) = 8760 \sum_{i=1}^{N_d} \rho_i \sum_{j=1}^{N_t} \left[\int_{v_{\mathrm{in}}}^{v_{\mathrm{out}}} f_i(v) P(v_j) dv\right] \quad (6)$$

where 8760 is the total hours per year, N_d is the number of wind sectors on the wind rose, ρ_i is the probability of the ith wind
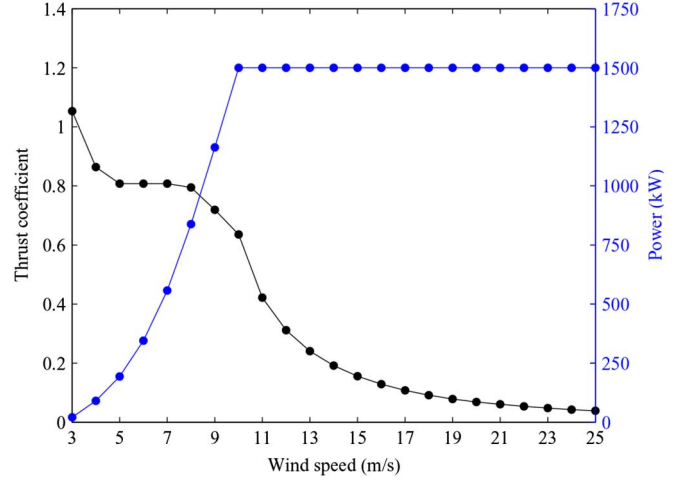
direction, v_{in} and v_{out} are respectively the cutin and cutout speeds defined in the turbine power curve, and $P(v_j)$ is the power produced by the jth turbine according to its power curve at the incident speed v_j. The incident speed v_j accounts for the topographic speedup and the wake deficit, and is derived from the free stream wind speed v at the hub height.

In this paper, the cost of access roads is assumed to be proportional to their length. Given N_t the number of turbines, their rated power P_{rate}, and the total length $L_{\mathrm{RN}}(\boldsymbol{z})$ of the road network, the following net present value function $\mathrm{NPV}(\boldsymbol{z})$ is defined to measure the profitability of a wind farm project throughout its life span T [2]

$$\begin{aligned}
\mathrm{NPV}(\boldsymbol{z}) = {} & -N_t \cdot P_{\mathrm{rate}} \cdot C_{\mathrm{WT}} - L_{\mathrm{RN}}(\boldsymbol{z}) \cdot C_{\mathrm{RN}} \\
& + \sum_{k=1}^{T} \frac{\mathrm{AEP}(\boldsymbol{z}) \cdot k_{\mathrm{RF}} \cdot p_{\mathrm{kWh}} \cdot (1 + \Delta p_{\mathrm{kWh}})^{k+1}}{(1+r)^k} \\
& - \sum_{k=1}^{T} \frac{\mathrm{AEP}(\boldsymbol{z}) \cdot k_{\mathrm{RF}} \cdot p_{\mathrm{OM}} \cdot (1 + \Delta p_{\mathrm{OM}})^{k+1}}{(1+r)^k}
\end{aligned}$$

$$(7)$$

where C_{WT} is the turbine cost per kilowatt, C_{RN} is the road network cost per meter, k_{RF} is the reliability factor takes into account the turbine downtime associated with both scheduled and unscheduled maintenance [26], p_{kWh} is the energy sale price per kilowatt-hour, Δp_{kWh} is the annual increase in the energy sale price, p_{OM} is the operation and maintenance cost per kilowatt-hour [26], Δp_{OM} is the annual increase in operation and maintenance cost, and r is the interest rate. Due to the complexity of the power transformation system and its cable network, the electrical system is not considered in this paper.

IV. SIMULATION RESULTS AND ANALYSES

The wind turbine UP1500-86 [27] from Guodian United Power, China is used in simulations. The rotor diameter of the wind turbine is 86 m, and the hub height is 80 m. The corresponding thrust coefficient curve and power curve of the wind turbine are shown in Fig. 4. The topography of the wind farm is
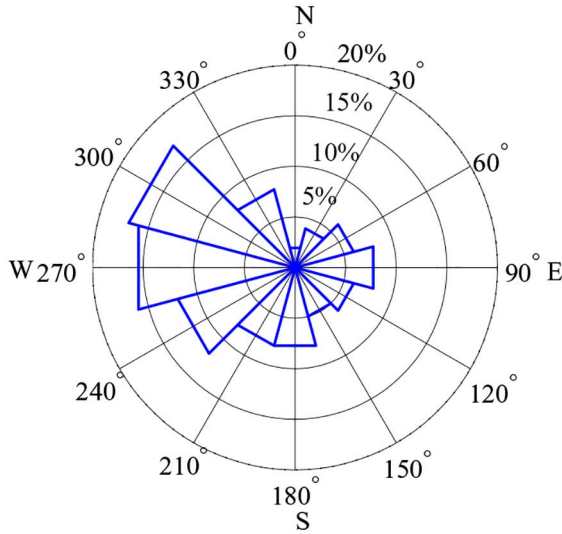
Fig. 5. Wind rose [28].

TABLE II
WIND DISTRIBUTION PARAMETERS [28]

Direction	Frequency	Scale parameter	Shape parameter
0°	0.020	6.4	1.79
30°	0.044	7.4	1.81
60°	0.056	8.8	1.65
90°	0.076	7.0	1.96
120°	0.061	7.3	1.83
150°	0.053	7.5	1.81
180°	0.078	8.0	1.89
210°	0.083	8.9	1.85
240°	0.123	9.8	1.96
270°	0.158	9.9	1.92
300°	0.167	9.3	1.93
330°	0.079	7.8	1.75

TABLE III
VARIABLES AND PARAMETERS OF THE COST FUNCTION [3], [26]

Variables	Descriptions	Values	Units
C_{RN}	Road network cost	200	€/m
C_{WT}	Wind turbine cost	800	€/kW
ΔC_{OM}	Yearly increase of O&M cost	6%	—
Δp_{kWh}	Yearly increase of energy price	3%	—
k_{RF}	Wind turbine reliability factor	95%	—
N_t	The number of wind turbines	26	—
p_{kWh}	Price of energy	0.07	€/kWh
p_{OM}	O&M cost per kilowatt-hour	0.004	€/kWh
P_{rate}	Turbine rated power	1.5	MW
r	Interest rate	6%	—
T	Life span	20	year

set to 350 m (slightly longer than four times rotor diameters). The computational domain $2450 \times 2450 \, \text{m}^2$ is partitioned into 7×7 cells. A turbine layout solution is encoded by a binary string of length 49, and each bit in the string represents whether the cell is chosen as a potential turbine location. The string or an individual solution indicates the number and locations of turbines.

The genetic algorithm repeatedly modifies a population of individual solutions. At each iteration, three main types of rules are used to create the next generation from the current population [30]: 1) selection rules select the individuals, called parents, that contribute to the population at the next generation; 2) crossover rules combine two parents to form children for the next generation; 3) mutation rules apply random changes to individual parents to form children, in order to avoid the trap of local minima and maintain diversity in the population. Over successive generations, the population "evolves" toward an optimized solution.

The genetic algorithm in MATLAB global optimization toolbox is used for simulations. The number of variables is 49, the population type "Bit string," the population size $N_{pop} = 50$, the number of generations $N_{gen} = 100$, the selection rule "Roulette," the crossover rule "Scattered" with the crossover probability 0.8, and the type of mutation "Uniform" with the mutation probability 0.08. The other parameters are set as default. Fig. 6 shows the block diagram of the optimization procedures of wind farm micrositing.

B. Case Study

Two comparative cases are studied to investigate the effectiveness of the proposed road network design model and the significance of road network optimization for farms in hills or mountains. Due to the randomness of genetic algorithms, ten independent runs are performed for each case. Table IV summarizes the results, including the best, average, and worst values of the best solutions achieved in each independent run.

In Case 1, the micrositing problem is solved in a two-stage manner, i.e., we first search for an optimized turbine layout *without considering access roads* and then design the road network for the given layout. The best configuration of the wind farm is shown in Fig. 7, where the blue triangle represents the entrance of the wind farm, red points mean the locations of

shown in Fig. 2(a) and its surface roughness length z_0 is 0.7 m [25]. Wind direction and speed distributions at 80 m above ground level at the mast location (represented by a blue triangular in Fig. 7) are shown in Fig. 5 and Table II. The wind resource grid is calculated by WAsP according to the farm topology, the wind speed and direction distributions of the measurement mast.

The road gradient g_r is limited to be no lager than 5% [29] to accommodate heavy vehicles for wind turbine installation. The variables and parameters of the cost function are shown in Table III. The micrositing objective is to find the optimal turbine layout z so as to maximize the net present value $\text{NPV}(z)$

$$\max \text{NPV}(z).$$

A. Optimization Algorithm

The genetic algorithm proposed in [6] and [7] is used as the layout optimizer. The wind farm is equally divided into several cells, in the center of which turbines could be placed. Since the Park wake model is only valid when distances between neighboring turbines are longer than approximately four rotor diameters [23], [24], the width of each cell in this paper is

TABLE IV
STATISTICS ON SIMULATION RESULTS (10 INDEPENDENT SIMULATIONS FOR EACH CASE)

Variables	Case 1			Case 2		
	Best	Average	Worst	Best	Average	Worst
Net present value $\mathrm{NPV}(z)$ (M€)	114.60	114.40	114.24	114.90	114.60	114.35
The length of the road network L_{RN} (km)	18.10	18.46	18.83	16.47	16.67	16.74
Road network cost (M€)	3.62	3.69	3.77	3.29	3.33	3.45
Wind turbine cost (M€)	31.20	31.20	31.20	31.20	31.20	31.20
Initial investment (M€)	34.82	34.89	34.97	34.49	34.53	34.65
Annual energy production $\mathrm{AEP}(z)$ (GWh)	157.82	157.69	157.60	157.79	157.60	157.27
Time*(h)	7.40	7.12	6.86	8.85	9.72	9.75

*Running MATLAB parallel computing in IBM Blade Center HS22 with 12 Intel Xeon X5650 CPUs (12 M Cache, 2.66 GHz, 6.40 GT/s Intel QPI) and 24 GB RAM.
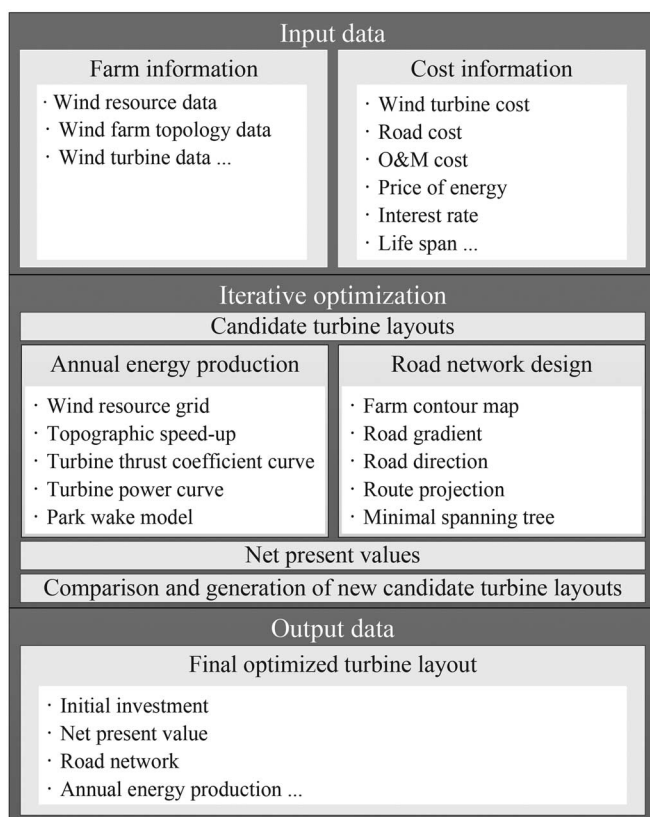

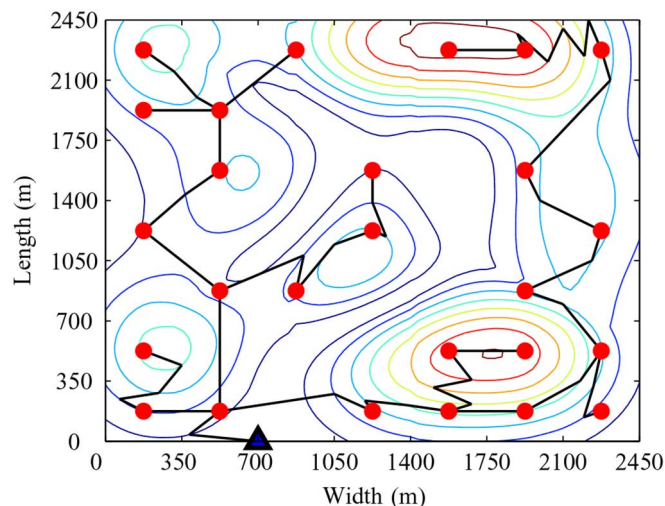Fig. 6. Block diagram of wind farm micrositing optimization.

Fig. 7. Best wind farm configuration of Case 1.

technique, the running time for each simulation is still around 7–10 h.

For both turbine layouts, reasonable road networks with feasible winding roads are obtained, which demonstrates the effectiveness of the proposed road network design model. Comparing Figs. 7 and 8, it is clear that the configuration of the road network depends on the turbine layout and the farm topology considerably. Therefore, to create a cost-effective road network, it is necessary to consider these two parts simultaneously during the microsting optimization process. Indeed, since the road network is simultaneously considered in Case 2, while the cost of the road network is ignored in Case 1, Case 2 consistently has a higher net present value than Case 1 in all independent runs. In the simulations, the net present value is determined by the annual energy production and the length of the road network. According to Table IV, one should choose a more cost-effective road network in order to further increase the net present value, when the annual energy production cannot be significantly improved (reaching the limit). Furthermore, the road-network length of Case 2 is decreased by over 9% in comparison to Case 1 for all independent runs, which will result in a short wind farm construction period and less impact to the local environment. Note that, $N_{\mathrm{pop}} \times N_{\mathrm{gen}} = 5000$ road networks need to be designed during the micrositing optimization process and the required computation time increases by around

wind turbines, and black polylines are the designed road network. In Case 2, the turbine layout and its corresponding road network are optimized simultaneously, i.e., in each optimization iteration, the road network design model is performed for every individual turbine layout generated by the genetic algorithm. The best configuration of the wind farm is shown in Fig. 8. The simulation results of both cases are summarized in Table IV.

Note that, the simulations for both cases are time consuming. The simulations were carried out in an IBM Blade Center HS22 with 12 Intel Xeon X5650 CPUs at a frequency 2.66 GHz. Parallel computing was employed to speed up the simulation progress. In each run of the 10 independent simulations, 12 CPUs were utilized simultaneously and each CPU was responsible for each wind direction. Even with the parallel computing
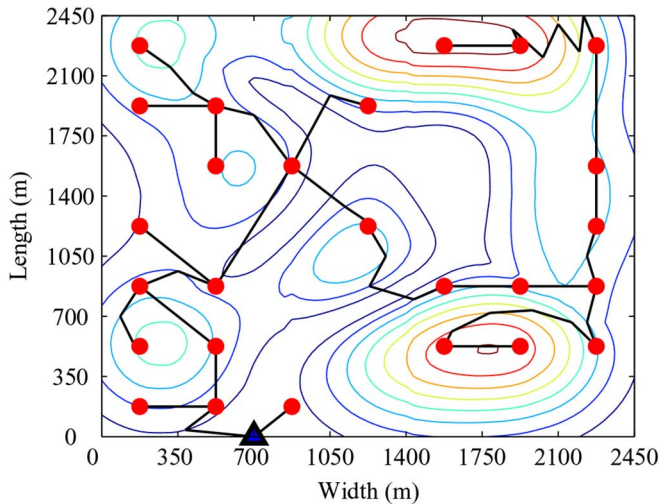
Fig. 8. Best wind farm configuration of Case 2.

36% on average. In summary, considering road network during the micrositing optimization can achieve a more practical and profitable wind farm planning.

The automatic model of road network design quickly evaluates a large number of alternative road networks corresponding to different turbine layouts yielded by evolutionary algorithms during the searching process. Although it is not designed to optimize the final route locations at an operational level, it forms the foundation for a final design of access roads.

V. Conclusion and Future Work

In this paper, a fast road-network design approach is developed to help micrositing engineers simultaneously optimize the turbine layout and its corresponding road network for hilly or mountainous wind farms. The route projection on contour maps is mathematically formulated with a gradient-bounded algorithm to design the preliminary road between any two wind turbines. The contour tree is applied to deduce the road direction for automating the route projection process. The minimum spanning tree is introduced to find the most cost-effective road network. Since the road network depends on the turbine layout and the farm topology, it is vital to simultaneously optimize turbine layout and the associated road network in order to further increase net present value of the wind farm, reduce farm construction period and environmental damages. As illustrated in two comparative cases, the proposed method results in a more practical and profitable turbine layout demonstrating the importance of road network optimization.

The main advantage of the proposed accessing road design model is that it is fast enough to be incorporated into the micrositing optimization progress that needs hundreds or thousands of iterations and is itself time consuming. The optimized assessing roads and the layout of wind turbines are primarily used at the initial stage of road planning and turbine micrositing. The turbine layout can be further improved by some techniques such as allowing each turbine to adjust its position within the given cell. Once the turbine positions are determined,

commercial software in civil engineering can be employed to finalize the smooth road network.

Besides road construction, the proposed method can potentially be applied to investigate the influence of electrical cable network on wind farm micrositing, since electrical cables are laid out underground to connect the wind farm power transformation system. Moreover, Euclidean Steiner tree may be introduced in the future to further decrease the length of the road network. As the implementation of Euclidean Steiner tree is based on digital elevation model rather than contours, it usually takes much more time to search for a relatively shorter road. It will be of great importance to improve the efficiency of the Euclidean Steiner tree for its application to wind farm road design.

References

[1] S. Zhao and R. Li, "Study on wind power generation cost in Zhejiang: Analysis of wind farm construction cost," East China Invest. Des. Inst. CHECC, Tech. Rep., 2009 [Online]. Available: http://www.cresp.org.cn/uploadfiles/114/1664/a2-b11-cs-2007-007-2-en.pdf

[2] J. Serrano González, A. G. Gonzalez Rodriguez, J. Castro Mora, J. Riquelme Santos, and M. Burgos Payan, "Optimization of wind farm turbines layout using an evolutive algorithm," Renew. Energy, vol. 35, no. 8, pp. 1671–1681, 2010.

[3] J. Serrano González, A. G. González Rodríguez, J. Castro Mora, M. Burgos Payán, and J. Riquelme Santos, "Overall design optimization of wind farms," Renew. Energy, vol. 36, no. 7, pp. 1973–1982, 2011.

[4] M. Munday, G. Bristow, and R. Cowell, "Wind farms in rural areas: How far do community benefits from wind farms represent a local economic development opportunity?" J. Rural Stud., vol. 27, pp. 1–12, 2011.

[5] "Renewable energy technologies: Cost analysis series," Int. Renew. Energy Agency, Tech. Rep., 2012, vol. 1, no. 5/5 [Online]. Available: http://www.irena.org/DocumentDownloads/Publications/RE_Technologies_Cost_Analysis-WIND_POWER.pdf

[6] G. Mosetti, C. Poloni, and B. Diviacco, "Optimization of wind turbine positioning in large wind farms by means of a genetic algorithm," J. Wind Eng. Ind. Aerodyn., vol. 51, no. 1, pp. 105–116, 1994.

[7] S. A. Grady, M. Y. Hussaini, and M. M. Abdullah, "Placement of wind turbines using genetic algorithms," Renew. Energy, vol. 30, no. 2, pp. 259–270, 2005.

[8] M. Song, K. Chen, Z. He, and X. Zhang, "Bionic optimization for micro-siting of wind farm on complex terrain," Renew. Energy, vol. 50, pp. 551–557, 2013.

[9] M. Song, K. Chen, Z. He, and X. Zhang, "Optimization of wind farm micro-siting for complex terrain using greedy algorithm," Energy, vol. 67, pp. 454–459, 2014.

[10] C. Wan, J. Wang, G. Yang, H. Gu, and X. Zhang, "Wind farm micro-siting by Gaussian particle swarm optimization with local search strategy," Renew. Energy, vol. 48, pp. 276–286, 2012.

[11] P. Fagerfjäll, "Optimizing wind farm layout - more bang for the buck using mixed integer linear programming," Master's thesis, Dept. Math. Sci., Chalmers Univ. Technol., Gothenburg Univ., 2010 [Online]. Available: http://www.math.chalmers.se/Math/Research/Optimization/reports/masters/Fagerfjall-final.pdf

[12] K. Nassar, M. E. Masry, and H. Osman, "Simulating the effect of access road route slection on wind farm construction," in Proc. 2010 Winter Simul. Conf., 2010, pp. 3272–3282 [Online]. Available: http://ieeexplore.ieee.org/xpl/login.jsp?tp=&arnumber=5679019&url=http%3A%2F%2Fieeexplore.ieee.org%2Fxpls%2Fabs_all.jsp%3Farnumber%3D5679019

[13] A. E. Akay, "A new method of designing forest roads," Turkish J. Agric. For., vol. 28, no. 4, pp. 273–279, 2004.

[14] K. Aruga, J. Sessions, and A. E. Akay, "Heuristic planning techniques applied to forest road profiles," *J. For. Res.*, vol. 10, no. 2, pp. 83–92, 2005.

[15] K. Aruga, "Tabu search optimization of horizontal and vertical alignments of forest roads," *J. For. Res.*, vol. 10, no. 4, pp. 275–284, 2005.

[16] B. Pérez, R. Mínguez, and R. Guanche, "Offshore wind farm layout optimization using mathematical programming techniques," *Renew. Energy*, vol. 53, pp. 389–399, 2013.

[17] L. W. Rogers, "Automating contour-based route projection for preliminary forest road designs using GIS," Master's thesis, Coll. Forest Resour., Univ. Washington, Seattle, WA, USA, 2005 [Online]. Available: http://www.ruraltech.org/pubs/theses/lwrogers/lwrogers_ms_thesis.pdf

[18] J. Chen, C. Qiao, and R. Zhao, "A voronoi interior adjacency-based approach for generating a contour tree," *Comput. Geosci.*, vol. 30, no. 4, pp. 355–367, 2004.

[19] C. Huang and T. Shih, "On the complexity of point-in-polygon algorithms," *Comput. Geosci.*, vol. 23, no. 1, pp. 109–118, 1997.

[20] R. Prim, "Shortest connection networks and some generalizations," *Bell Syst. Tech. J.*, vol. 36, pp. 1389–1401, 1957.

[21] AWS Truepower, LLC. (2010, Apr.). OpenWind theoretical basis and validation [Online]. Available: https://www.awstruepower.com/assets/Open WindTheoryAndValidation_v1p3_Apr2010.pdf

[22] N. G. Mortensen, D. N. Heathfield, L. Myllerup, L. Landberg, and O. Rathmann. (2007, Jun.). Getting started with WAsP 9 [Online]. Available: http://www.wasp.dk/~/media/Sites/WASP/WAsP%20support/ Getting%20Started%20with%20WAsP%209.ashx

[23] N. O. Jensen, "A note on wind generator interaction," Risø Natl. Lab., Roskilde, Denmark, Tech. Rep. Riso-M-2411, 1984 [Online]. Available: http://www.risoe.dk/rispubl/vea/veapdf/ris-m-2411.pdf

[24] I. Katic, J. Højstrup, and N. O. Jensen, "A simple model for cluster efficiency," in *Eur. Wind Energy Assoc. Conf. Exhib.*, Rome, Italy, 1986, vol. 1, pp. 407–410.

[25] T. Burton, D. Sharpe, N. Jenkins, and E. Bossanyi, *Wind Energy Handbook*. Hoboken, NJ, USA: Wiley, 2001.

[26] C. A. Walford, "Wind turbine reliability: Understanding and minimizing wind turbine operation and maintenance costs," Sandia Natl. Lab., Albuquerque, NM, USA, Tech. Rep. SAND2006-1100, 2006.

[27] Guodian United Power Technology. (2013). "Wind turbine UP1500-86," [Online]. Available: http://www.gdupc.com.cn/newsDetailEN. aspx?id=14325

[28] H. Gu and J. Wang, "Irregular-shape wind farm micro-siting optimization," *Energy*, vol. 57, pp. 535–544, 2013.

[29] F. Miceli. (2013). "Maximum wind farm internal road gradient," [Online]. Available: http://www.windfarmbop.com/maximum-road-grade/

[30] *Global Optimization Toolbox User's Guide*. MATLAB help, The Math-Works, Natick, MA, USA, 2014 [Online]. Available: http://www.mathworks.com/help/pdf_doc/gads/gads_tb.pdf

Jun Wang (S'98–M'03–SM'12) received the B.E. degree from Hefei University of Technology, Hefei, China, in 1996, the M.E. degree from the Southeast University, Nanjing, China, in 1999, and the Ph.D. degree from the University of Leeds, Leeds, U.K., in 2003, all in control engineering.

He was a Postdoctoral Research Fellow in Control Science and Engineering with Tsinghua University, Beijing, China, from 2003 to 2005, and the Deputy Director with the Laboratory Center of Automation Education, Tsinghua University, from 2006 to 2010. He has been the Professor in Control Engineering with the Department of Control Science and Engineering, Tongji University, Shanghai, China, since September 2010, and the Head of the Department since January 2014. His research interests include robust control, multiobjective control, artificial intelligence theory and their applications to the areas of vehicle dynamics, and renewable energy.

Dr. Wang was a Guest Editor of the *International Journal of Vehicle Design*.

Qin Lin received the B.E. degree in automation from Hefei University of Technology, Hefei, China, in 2011, and the M.E. degree in control theory and control engineering from Tongji University, Shanghai, China, in 2014.

His research interests include data mining, signal processing theory and their applications to wind power prediction, and wind energy resource assessment.

Qi Gong received the B.E. degree in automation from Dalian University of Science and Technology, Dalian, China, in 1996, the M.E. degree in automatic control from Southeast University, Nanjing, China, in 1999, and the Ph.D. degree in electrical engineering and computer science from Case Western Reserve University, Cleveland, OH, USA, in 2004.

Currently, he is an Associate Professor with the Department of Applied Mathematics and Statistics, University of California, Santa Cruz, CA, USA. His research interests include computational optimal control, trajectory optimization, nonlinear control systems, and industry control applications.

Dr. Gong received the Postdoctoral Research Associateship Award from the National Research Council in 2004.

Huajie Gu received the B.E. degree in automation from Nanjing Technical University, Nanjing, China, in 2011, and the M.E. degree in control theory and control engineering from Tongji University, Shanghai, China, in 2014.

His research interests include stochastic algorithms, image processing, pattern recognition, computational fluid dynamics, and their applications to renewable energy.